Boundary height fields in the Abelian sandpile model

2005 J. Phys. A: Math. Gen. 38 1451

(http://iopscience.iop.org/0305-4470/38/7/004)

INSTITUTE OF PHYSICS PUBLISHING JOURNAL OF PHYSICS A: MATHEMATICAL AND GENERAL

J. Phys. A: Math. Gen. **38** (2005) 1451–1472 doi:10.1088/0305-4470/38/7/004

Boundary height fields in the Abelian sandpile model

Geoffroy Piroux and Philippe Ruelle

Institut de Physique Théorique, Université Catholique de Louvain,
B-1348 Louvain-La-Neuve, Belgium

E-mail: piroux@fyma.ucl.ac.be and ruelle@fyma.ucl.ac.be

Received 4 October 2004, in final form 14 December 2004
Published 2 February 2005
Online at stacks.iop.org/JPhysA/38/1451

Abstract

We study the Abelian sandpile model on the upper half-plane, and reconsider the correlations of the four height variables lying on the boundary. For more convenience, we carry out the analysis in the dissipative (massive) extension of the model and identify the boundary scaling fields corresponding to the four heights. We find that they all can be accounted for by the massive pertubation of a $c = -2$ logarithmic conformal field theory.

PACS numbers: 45.70.Cc, 05.70.Jk, 11.25.Hf

1. Introduction

The description of equilibrium critical phenomena has been one of the greatest successes of two-dimensional conformal theories in the past 20 years [1]. More recently, attention has focused on new types of observables in otherwise well-known models, and also on new kinds of critical systems. In both cases, non-local features often play an important role, because either the observables one is interested in are themselves non-local in terms of the natural microscopic variables, or else because the statistical model possesses intrinsic non-local properties. These studies often lead to a description in terms of conformal theories with peculiar properties. A class of systems with such properties is provided by sandpile models. Some of them, and in particular the one we consider here, are believed to have a faithful description in terms of logarithmic conformal field theories.

Our motivation to study these models is twofold. First, one wishes to see to what extent they lend themselves to a conformal field theoretic approach, and if the adequacy of the conformal description is as good as for the equilibrium systems. Second, the logarithmic theories have been developed for themselves, but are complex and some of their aspects are not fully understood yet. It should therefore be profitable to have concrete realizations in order to have a better understanding of the most peculiar features.

The sandpile model we consider here is the isotropic Abelian sandpile model (ASM), as originally defined in [2]. The most natural variables to consider in a conformal context are the

four height variables. In the bulk, correlations of height 1 variables can be handled by local calculations [3], but height 2, 3 and 4 variables are much more complicated, and only their one-site probabilities are known [4]. For sites on a boundary, closed or open, Ivashkevich showed, by using suitable identities, that the non-local configurations needed to handle the heights bigger than 1 could be reduced to local computations [5]. He was then able to compute the two-site joint probabilities of all height variables. He found that all correlations decay like r^{-4}, and inferred, wrongly as we will see, that all boundary height variables scale to the same conformal field.

Our aim in this paper is to revisit this problem and to identify the fields corresponding to the boundary height variables, but in a dissipative extension of the model, known to be described by a massive perturbation of the $c = -2$ conformal theory [6]. The main advantage of doing this is that it allows for an unambiguous identification of the fields from a few 2-point correlators, off, and therefore also at, criticality. The so-obtained identification can then be checked from other 2-point and from 3-point functions. In contrast, when one considers the critical, non-dissipative model, the 2-point functions yield ambiguous field identifications, which can only be fixed by using 3-point functions, and then checked from higher correlators.

The paper is organized as follows. The next section defines the model and sets our conventions. Section 3 deals with the boundary unit height variable and what we call supercritical height variables. They are much easier than the other ones, and illustrate the way the identification with concrete fields is obtained. The identification of the height 1 and supercritical height fields also facilitates that of the other heights.

Sections 4 and 5 form the hardcore of this paper. In section 4, we explain our prescription—a two-step burning algorithm—to associate recurrent configurations of the sandpile with spanning trees, from which a clear characterization of the local height constraints follows. We use it to compute two-site probabilities for having a height 1 or a supercritical height at one site, and any other height at the other site, from which we deduce the field identification of all height variables. Section 5 checks these results by computing explicitly all two-site height probabilities in the massive extension of the sandpile model, and certain three-site probabilities involving a height 1 or a supercritical height.

Since the bulk of the calculations reported here was done, an article by Jeng [7] has appeared, where precisely the same problem is addressed. The two works were carried out independently and differ in two ways. The first one is that we study the dissipative model, while Jeng considers it at criticality. This fact enables us to deduce the field identifications for the boundary height variables $h > 1$ from the spanning tree characterizations of a single insertion of such variables, technically much simpler to solve than the two-site insertions. The latter are only used as cross-checks, in contrast to the approach at criticality which needs them as inputs. So working off criticality offers a simpler and more reliable access to the fields. Secondly, we use a different characterization of the height variables bigger or equal to 2 in terms of spanning trees, which is based on a modified, two-step burning algorithm. This, we believe, leads to a more transparent formalism which generalizes to multisite probabilities. Our results and conclusions however fully agree with those of Jeng.

2. The dissipative sandpile model

Consider a finite portion $\mathcal{L}$ of a square lattice and define at each site i, a (sand) height variable h_i which can take the integer values $1, 2, 3, \ldots$. A configuration $\mathcal{C}$ of the sandpile is the set of height values $\{h_i\}$ for all sites. The dynamics is defined in terms of a symmetric toppling matrix Δ. Its entries are all integers, positive on the diagonal, negative off the diagonal, and

it has row sums which are non-negative. A configuration is called stable if all heights satisfy $h_i \leqslant \Delta_{ii}$.

The system evolves in discrete time as follows. To the stable configuration $\mathcal{C}_t$ at time t we add a sand grain at a random site i (chosen with uniform distribution say), namely we set $h_i \to h_i + 1$. This new configuration, if stable, defines $\mathcal{C}_{t+1}$. If it is not stable, the unstable site i topples: it loses Δ_{ii} grains, every other site j receives $-\Delta_{ij}$ grains, whereas $\sum_{j\in\mathcal{L}} \Delta_{ij}$ sand grains are dissipated (they fall off the pile, to a sink). That is, when a site i topples, we update the heights according to

$$h_j \longrightarrow h_j - \Delta_{ij}, \qquad \forall j \in \mathcal{L}. \tag{1}$$

If other sites become unstable after the toppling of the site i, they topple following the same rule. All unstable sites are then toppled until the configuration becomes stable again. This configuration is then taken as $\mathcal{C}_{t+1}$. In this way, the toppling at the seeded site can trigger a potentially large avalanche, resulting in a configuration $\mathcal{C}_{t+1}$ which can be completely different from $\mathcal{C}_t$.

Provided there are dissipative sites, i.e. sites k for which $\sum_{j\in\mathcal{L}} \Delta_{kj} > 0$, the dynamics is well defined: it does not depend on the order in which the sites are toppled (the model is Abelian), and the relaxation of the seeded configuration to $\mathcal{C}_{t+1}$ requires a finite number of topplings.

One is generally interested in the long-time behaviour of the sandpile. As shown by Dhar [8], this behaviour is characterized by a unique time invariant probability measure $P^*_{\mathcal{L}}$, which specifies the probabilities of occurrence of all stable configurations, independently of the initial configuration. The moments of this measure, in the thermodynamic limit $|\mathcal{L}| \to \infty$, are what we want to put in correspondence with the correlators of a conformal field theory.

When the dynamics is started from a certain initial configuration, it produces at later times two kinds of configurations, called transient and recurrent in the terminology of Markov processes. The transient configurations are those which occur a finite number of times only (they may not occur at all, depending on the initial configuration). In the long run, they are not in the image of the dynamics, and have a zero measure with respect to $P^*_{\mathcal{L}}$. A simple example is the configuration with all $h_i = 1$, but more generally, any configuration with two 1 at neighbour sites (sites i, j with $\Delta_{ij} \neq 0$) is transient.

The non-transient configurations are recurrent. Their number is equal to $\det\Delta$, the determinant of the toppling matrix, and asymptotically, they occur with equal probability, so that the measure $P^*_{\mathcal{L}}$ is uniform on them [8]. A criterion to decide whether a given configuration is recurrent or transient is based on the notion of forbidden sub-configuration (FSC): a sub-configuration, with support $\mathcal{K} \subset \mathcal{L}$, is said to be forbidden if $h_i \leqslant -\sum_{j\in\mathcal{K}\setminus\{i\}} \Delta_{ji}$, for all sites i of $\mathcal{K}$. For instance two neighbour sites with heights 1 form an FSC. Then a configuration is recurrent if and only if it contains no FSC [9].

A practical way to test a configuration is to use the burning algorithm [8]. At time 0, all sites in $\mathcal{L}$ are unburnt and we define $\mathcal{K}_0 = \mathcal{L}$ to be the set of unburnt sites at time 0. The sites i of $\mathcal{K}_0$ such that $h_i > -\sum_{j\in\mathcal{K}_0\setminus\{i\}} \Delta_{ji}$ are burnable at time 1. So we burn them, obtaining a smaller set $\mathcal{K}_1 \subset \mathcal{K}_0$ of unburnt sites at time 1. Then the sites of $\mathcal{K}_1$ which are burnable at time 2, i.e. those satisfying $h_i > -\sum_{j\in\mathcal{K}_1\setminus\{i\}} \Delta_{ji}$, are burnt. This leaves a smaller set $\mathcal{K}_2 \subset \mathcal{K}_1$ of unburnt sites at time 2. This burning process is carried on until no more sites are burnable, which means that $\mathcal{K}_{T+1} = \mathcal{K}_T$ for a certain T. Then the configuration is recurrent if and only if all sites of $\mathcal{L}$ have been burnt ($\mathcal{K}_T = \emptyset$). Otherwise $\mathcal{K}_T$ is an FSC.

The burning algorithm allows us to define a unique rooted spanning tree on a graph $\mathcal{L}^\star$, from the path followed by the fire in the lattice [9]. The graph $\mathcal{L}^\star$ has the sites of $\mathcal{L}$ and the sink as vertices, and has links defined by Δ: an off-diagonal entry $\Delta_{ij} = -n$ means there are

n bonds connecting the sites i and j, and each site i is connected to the sink by a number of bonds equal to $\sum_{j\in\mathcal{L}} \Delta_{ij} \geqslant 0$, the number of grains dissipated when i topples. At time 0, the sink is the only burnt site and forms the root of the tree. In the next steps, the fire propagates from the sink to those sites which are burnable at time 1, then from the sites which have been burnt at time 1 to those which are burnable at time 2, and so on. If a site burns at time t, one says that it catches fire from one among its neighbours that were burnt at time $t-1$ (or from the sink site at time 1). In case there are more than one of these, a fixed ordering prescription is used to decide along which bond the fire actually propagates. (The precise prescription will not be needed in what follows; the interested reader is referred to [9] for an example of such a prescription.) The collection of all bonds forming the fire path defines a spanning tree, rooted in the sink, and growing towards the interior of the lattice $\mathcal{L}$.

This improved algorithm establishes a correspondence between the set of recurrent configurations on $\mathcal{L}$ and the set of rooted spanning trees on $\mathcal{L}^\star$. The precise mapping, although one-to-one, however depends on the prescription used. The prescription we will use below differs slightly from the one defined in [9], but is equally valid. The specific sandpile model we consider in the next sections is defined on the discrete upper half-plane $\mathcal{L} = \mathbb{Z}_> \times \mathbb{Z}$, and has the massive discrete Laplacian as toppling matrix subjected to the two different boundary conditions 'open' and 'closed' on the boundary, which we take to be the line $y = 1$. The two toppling matrices are almost identical and differ only along the boundary. They both depend on a positive parameter t, controlling the rate at which sand is dissipated when sites topple. They read explicitly

$$\Delta^{\mathrm{op}}_{ij} = \begin{cases} 4+t & \text{if} \quad i=j, \\ -1 & \text{if} \quad i \text{ and } j \text{ are n.n.}, \\ 0 & \text{otherwise}, \end{cases} \qquad \Delta^{\mathrm{cl}}_{ij} = \begin{cases} 4+t & \text{if} \quad i=j \text{ are off boundary}, \\ 3+t & \text{if} \quad i=j \text{ are on boundary}, \\ -1 & \text{if} \quad i \text{ and } j \text{ are n.n.}, \\ 0 & \text{otherwise}. \end{cases} \tag{2}$$

One easily sees that t grains of sand are dissipated (transferred to the sink) each time a site topples, or $t+1$ if it is an open boundary site that topples. This model will be called the massive Abelian sandpile model (MASM) in reference to the massive discrete Laplacian where $\sqrt{t}$ plays the role of a mass. The usual, critical model originally defined in [2], is recovered at $t = 0$.

In terms of the graph $\mathcal{L}^\star$, bulk sites and closed boundary sites have a t-fold connection to the sink, while open boundary sites have a $(t+1)$-fold connection to it. In addition, all nearest neighbour (n.n.) sites on $\mathcal{L}$ are connected by a single bond.

An easy corollary of the above burning algorithm is that a site with height smaller or equal to the number of its neighbours on $\mathcal{L}$ (3 or 4) is never burnt at time 1, and therefore catches fire from one of its neighbours and not from the sink. Conversely, a site with height strictly larger than $\Delta_{ii} - t$, which we call a *supercritical height*, or an open boundary site with $h = 4$ is set afire by the sink. Supercritical height values are those which exist only when t is nonzero.

According to the definition of Δ, t should take integer values. However the MASM correlations decay exponentially, with a correlation length that diverges only when t goes to 0, like $1/\sqrt{t}$ [10, 6]. The large distance limit of the lattice correlations must therefore be accompanied by a small t limit, in such a way that their scaling limit $\sqrt{t} = Ma \to 0$, $|i-j| = |z|/a \to \infty$ be well defined when $a \to 0$. So in practice, one expands the lattice MASM correlations in powers of t, and selects the dominant terms[1]. These define correlators of a

[1] As has been noted on several occasions, a sandpile model with rational values of t can be defined, which is equivalent to the above one as far as the height variables are concerned, and in which the limit $t \to 0$ by rational values makes sense.

massive field theory, which, in this case, turns out to be a massive perturbation [6] of $c = -2$ logarithmic conformal theory [11–13],

$$S = \frac{1}{\pi}\int (\partial\theta\bar{\partial}\tilde{\theta} + M^2\theta\tilde{\theta}/4), \tag{3}$$

where $\theta, \tilde{\theta}$ are anticommuting scalar fields.

In the course of the calculations, we will make extensive use of the inverse toppling matrix Δ_{ij}^{-1}. As is well known, the inverse of Δ on the upper half-plane can be obtained in terms of the inverse massive Laplacian on the full plane Δ^{-1}, via the image method. For $i = (m_1, n_1)$ and $j = (m_2, n_2)$, the explicit formulae read

$$\begin{aligned} (\Delta^{\mathrm{op}})_{ij}^{-1} &= \Delta_{ij}^{-1} - \Delta_{ij^*}^{-1} = \Delta_{ij}^{-1} - \Delta_{i^*j}^{-1}, \qquad & j^* &= (m_2, -n_2), \\ (\Delta^{\mathrm{cl}})_{ij}^{-1} &= \Delta_{ij}^{-1} + \Delta_{ij^\vee}^{-1} = \Delta_{ij}^{-1} + \Delta_{i^\vee j}^{-1}, \qquad & j^\vee &= (m_2, 1 - n_2). \end{aligned} \tag{4}$$

The horizontal translation invariance is preserved in both cases, so that the entries of the inverse matrices depend on $|m_1 - m_2|$, n_1 and n_2. A short review on the values of the inverse massive Laplacian on the plane can be found in [6].

The lattice open boundary condition is identified with the Dirichlet condition in the continuum ($\theta = \tilde{\theta} = 0$ on $\mathbb{R}$), whereas the closed boundary condition corresponds to the Neumann condition ($\partial\theta - \bar{\partial}\theta = \partial\tilde{\theta} - \bar{\partial}\tilde{\theta} = 0$ on $\mathbb{R}$). The Lagrangian (3) then implies the following Green functions on the upper half-plane:

$$\langle\theta(z)\theta(w)\rangle = \langle\tilde{\theta}(z)\tilde{\theta}(w)\rangle = 0, \tag{5}$$

$$\langle\theta(z)\tilde{\theta}(w)\rangle_{\mathrm{op}} = K_0(M|z - w|) - K_0(M|z - \bar{w}|), \tag{6}$$

$$\langle\theta(z)\tilde{\theta}(w)\rangle_{\mathrm{cl}} = K_0(M|z - w|) + K_0(M|z - \bar{w}|), \tag{7}$$

where K_0 is the modified Bessel function.

3. Unit height and supercritical height variables

Multisite probabilities for a number of sites to have height equal to 1 or supercritical height values ($h_i > \Delta_{ii} - t$) is fairly easy if one uses the Bombay trick, a beautiful technique designed by Majumdar and Dhar [3]. It can be formulated in terms of height configurations or in terms of spanning trees. In this section, we will use it in terms of heights, the formulation with trees being a particular case of the general characterization given in the next section.

Suppose that we first want to compute the probability $P\left[h_{i_0} = 1\right]$ that a certain site i_0 has a height equal to 1. That probability is simply equal to the number of recurrent configurations with a height 1 at i_0 divided by the total number of recurrent configurations, which we know equals $\det\Delta$.

The idea of [3] is to define a new sandpile model in which the height at i_0 is always 1, and such that any recurrent configuration of this new model is in correspondence with a recurrent configuration of the original model where the height at i_0 is 1. To freeze the height at i_0 to the value 1, one simply reduces the diagonal entry of the toppling matrix to 1. So the toppling matrix Δ' of the new model will have $\Delta'_{i_0 i_0} = 1$. Then in the new model, the site i_0 will topple whenever its height exceeds 1, and each time it topples, it will lose a single grain which will go to a neighbour site or to the sink. Consequently, i_0 will have a single connection, either to the sink or to one of its neighbours in $\mathcal{L}$. Finally, the neighbours of i_0 cannot have a height equal to 1 in a recurrent configuration, so that they assume only $\Delta_{ii} - 1$ values. This can also be enforced in the new model by decreasing the diagonal entries of Δ by 1 for those neighbours

of i_0 which are no longer connected to i_0. As the connections fix the off-diagonal part of the toppling matrix, and the height ranges fix its diagonal part, this will determine Δ'.

Thus the number of recurrent configurations with a height 1 at i_0 is equal to the total number of recurrent configurations of the new model, itself equal to the determinant of the new toppling matrix Δ'. Setting $\Delta' = \Delta + B^{(i_0)}$, one obtains [3]

$$P\big[h_{i_0} = 1\big] = \frac{\det \Delta'}{\det \Delta} = \det(\mathbb{I} + \Delta^{-1} B^{(i_0)}), \tag{8}$$

where Δ is the toppling matrix appropriate to the boundary condition one considers. Because the difference $\Delta' - \Delta \equiv B^{(i_0)}$ is nonzero only on sites around i_0, the previous formula reduces to the calculation of a finite determinant, even on an unbounded lattice $\mathcal{L}$.

On the discrete upper half-plane, the defect matrix $B^{(i_0)}$ depends on the location of i_0. If i_0 is off the boundary, and if one keeps it connected to one of its four neighbours, then $B^{(i_0)}$ is equal to

$$B^{(i_0)} = \begin{pmatrix} -3-t & 1 & 1 & 1 \\ 1 & -1 & 0 & 0 \\ 1 & 0 & -1 & 0 \\ 1 & 0 & 0 & -1 \end{pmatrix} \tag{9}$$

on i_0 (first label) and any three neighbours of i_0, and is identically zero elsewhere (if the only connection of i_0 is to the sink, the B matrix is 5×5). In this case, the probability is given by a 4×4 determinant, and depends on the distance m of i_0 to the boundary. At the critical point ($t = 0$) and for large values of m, it is equal to [14]

$$P\big[h_{i_0} = 1\big] = P_1 \left[1 \pm \frac{1}{4m^2} + \cdots\right], \tag{10}$$

where the + (resp. −) sign refers to the open (resp. closed) boundary condition. $P_1 = 2(\pi - 2)/\pi^3 = 0.0736$ is the probability that a site deep inside the lattice (equivalently, on the infinite plane) has height 1 in the critical ASM.

If i_0 lies on the boundary, the matrix $B^{(i_0)}$ depends on the boundary condition and takes one of the two forms

$$B^{(i_0)}_{\mathrm{op}} = \begin{pmatrix} -3-t & 1 & 1 \\ 1 & -1 & 0 \\ 1 & 0 & -1 \end{pmatrix}, \qquad B^{(i_0)}_{\mathrm{cl}} = \begin{pmatrix} -2-t & 1 & 1 \\ 1 & -1 & 0 \\ 1 & 0 & -1 \end{pmatrix}. \tag{11}$$

The corresponding critical probability $P\big[h_{i_0} = 1\big]$ is then a constant, which only depends on the type of boundary the site i_0 is on [5],

$$P_1^{\mathrm{op}} = \frac{9}{2} - \frac{42}{\pi} + \frac{320}{3\pi^2} - \frac{512}{9\pi^3}, \qquad P_1^{\mathrm{cl}} = \frac{3}{4} - \frac{2}{\pi}. \tag{12}$$

The one-site probability $P\big[h_{i_0} = 1\big]$ can easily be computed for $t \neq 0$, but will not be needed in what follows.

The probability that a site be supercritical can be treated in a similar way, and is actually simpler. One now takes $t \neq 0$, since the probability does not make sense at $t = 0$.

Any site i_0, whatever its location and whatever the boundary condition, has t possible supercritical height values, namely $h = \Delta_{i_0 i_0} - t + 1, \ldots, \Delta_{i_0 i_0}$. The probability that a site i_0 has a fixed supercritical height h does not depend on h, because a recurrent configuration remains recurrent if one replaces a supercritical height at i_0 by another one. Therefore one has

$$P[i_0 \text{ is supercritical}] = P\big[h_{i_0} > \Delta_{i_0 i_0} - t\big] = t\, P\big[h_{i_0} = h\big], \tag{13}$$

where h is any fixed supercritical value.

It is actually easier to compute the probability that i_0 is not supercritical. To do that, one has to count the recurrent configurations with $h_{i_0} \leqslant \Delta_{i_0 i_0} - t$ ($=4$, or 3 on a closed boundary). In a new model defined by the new toppling matrix $\Delta'_{ij} = \Delta_{ij} - t\delta_{i,i_0}\delta_{j,i_0}$ on the same lattice, all recurrent configurations have i_0 not supercritical. One obtains

$$P[i_0 \text{ is supercritical}] = 1 - \frac{\det \Delta'}{\det \Delta} = t\,\Delta^{-1}_{i_0 i_0}, \tag{14}$$

and

$$P\big[h_{i_0} = h\big] = \Delta^{-1}_{i_0 i_0}. \tag{15}$$

The defect matrix method works here too, and is simpler because the appropriate matrix $\bar{S}^{(i_0)}_{ij} = -t\delta_{i,i_0}\delta_{j,i_0}$ has rank 1. The corresponding one-site probability is then given by a 1×1 determinant.

Let us note that the probabilities (15) are well defined for any strictly positive value of t, but behave badly in the critical limit $t \to 0$. For a closed boundary condition, they have a logarithmic singularity at $t = 0$. For an open boundary condition, they have a finite limit at $t = 0$, but which is not a probability in general: $\Delta^{-1}_{i_0 i_0} = 1 - 2/\pi = 0.3634$ for i_0 on the boundary, and then grows logarithmically with the distance of i_0 to the boundary.

So instead we will consider the probability (14) for a site or a collection of sites to be supercritical without specifying the actual heights. As we will see below, that observable has well-defined correlations in the massive scaling limit, and corresponds to a field that vanishes in the critical limit.

After the one-site probabilities, multisite probabilities and correlations can be computed by the same method almost routinely. The observables we consider in this section are the two boundary random variables $\delta(h_i - 1)$ and $\delta(i \text{ is supercritical})$ corresponding to the events 'i has height 1' or 'i is supercritical' for i a site on the boundary of the upper half-plane. In order to get fields whose expectation value vanishes infinitely far from the boundary, one considers the random variables subtracted by their average value. Anticipating the scaling dimension 2 or 4 of the above random variables, we define their scaling fields by

$$\begin{aligned} \phi_1^{\mathrm{op,cl}}(x) &= \lim_{a\to 0} \frac{1}{a^2}[\delta(h_{x/a} - 1) - P_1], \\ \phi_>^{\mathrm{op,cl}}(x) &= \lim_{a\to 0} \frac{1}{a^{4,2}}\big[\delta(h_{x/a} \text{ is supercritical}) - a^2 M^2 \Delta^{-1}_{\frac{x}{a}\frac{x}{a}}\big], \end{aligned} \tag{16}$$

subjected to the scaling relations $t = a^2 M^2$ and $i\sqrt{t} = Mx$.

To compute n-site probabilities, one simply inserts the proper defect matrices at the locations of the observables, so that the full defect matrix is a direct sum of n matrices $B^{(i)}$ or $\bar{S}^{(i)}$. One should however remember that $\bar{S}^{(i)}$ is not the defect matrix for i being supercritical but for i not being supercritical, the complementary event. The scaling limit of the latter gives rise to a field $\phi_\leqslant$, from which $\phi_> = -\phi_\leqslant$ is recovered. The probability then reduces to the calculation of a finite determinant whose entries are combinations of entries of the inverse toppling matrix. As the scaling limit takes t to zero, one expands these entries in power series of t, keeping only the dominant term. From (16) the latter yields the field theoretic correlation of fields ϕ_1 and $\phi_>$, which are then identified with explicit fields of the Lagrangian theory (3). This is a main advantage of working with the massive theory that this identification is essentially unambiguous.

The simplest way to proceed to the identification of the boundary fields ϕ_1 and $\phi_>$ is to use other lattice observables with already known field identifications. Examples of such observables are precisely the bulk version of the above two random variables. The

corresponding bulk fields have been identified in [6] (see also [15] for a proof that these identifications are consistent with a broad class of multisite correlations),

$$\phi_1(z) = -P_1\left[:\partial\theta\bar{\partial}\tilde{\theta} + \bar{\partial}\theta\partial\tilde{\theta}: + \frac{M^2}{2\pi}\,:\theta\tilde{\theta}:\right], \tag{17}$$

$$\phi_>(z) = \frac{M^2}{2\pi}\,:\theta\tilde{\theta}:\,. \tag{18}$$

One first computes the 2-point correlations involving one boundary observable and one bulk observable. From them, one may infer what the boundary fields must be, and then cross-check their form from other correlations. We do not give much detail as the calculations are fairly straightforward, but simply illustrate the method in a simple case, namely the identification of $\phi_>^{\rm op}(x)$ on an open boundary.

We take two reference sites, i_0 on the boundary and j_0 in the bulk, far from the boundary. The probability that they both are non-supercritical reduces to a rank 2 determinant

$$\begin{aligned} P[i_0,\, j_0 \text{ non-supercritical}] &= \frac{\det[\Delta^{\rm op} + \bar{S}^{(i_0)} + \bar{S}^{(j_0)}]}{\det \Delta^{\rm op}} \\ &= \det\begin{pmatrix} 1 - t(\Delta^{\rm op})^{-1}_{i_0 i_0} & -t(\Delta^{\rm op})^{-1}_{i_0 j_0} \\ -t(\Delta^{\rm op})^{-1}_{j_0 i_0} & 1 - t(\Delta^{\rm op})^{-1}_{j_0 j_0} \end{pmatrix}. \end{aligned} \tag{19}$$

Subtracting the product of disconnected probabilities obtained from (14), one has

$$P[i_0,\, j_0 \text{ non-supercritical}]_{\rm connected} = -t^2(\Delta^{\rm op})^{-2}_{i_0 j_0}. \tag{20}$$

If one chooses the two sites on a vertical line $i_0 = (0, 1)$ and $j_0 = (0, m)$, then (see, for instance, appendix A of [6])

$$(\Delta^{\rm op})^{-1}_{i_0 j_0} = \Delta^{-1}_{(0,1)(0,m)} - \Delta^{-1}_{(0,-1)(0,m)} = -\frac{\sqrt{t}}{\pi}K_0'(m\sqrt{t}) + \cdots \tag{21}$$

where the dots stand for subdominant terms in t. The dominant term in the connected two-site probability is thus

$$P[i_0,\, j_0 \text{ non-supercritical}]_{\rm connected} = -\frac{t^3}{\pi^2}K_0'^2(m\sqrt{t}) + \cdots. \tag{22}$$

Using the scaling relation (16), valid also for bulk fields (with a power a^{-2} for ϕ_1 and $\phi_\leqslant, \phi_>$), one finds the boundary/bulk 2-point function

$$\left\langle \phi_\leqslant^{\rm op}(x)\phi_\leqslant(x + {\rm i}y)\right\rangle = -\frac{M^6}{\pi^2}K_0'^2(My). \tag{23}$$

From the explicit form of $\phi_\leqslant(z) = -\frac{M^2}{2\pi}\,:\theta\tilde{\theta}:$ given above, one eventually arrives at

$$\left\langle \phi_\leqslant^{\rm op}(x)\,:\theta\tilde{\theta}:\,(x + {\rm i}y)\right\rangle = \frac{2M^4}{\pi}K_0'^2(My). \tag{24}$$

Using the Green function (6) on the upper half-plane with an open boundary, one sees that the only possible field assignment is $\phi_\leqslant^{\rm op}(x) = \frac{2M^2}{\pi}\,:\partial\theta\partial\tilde{\theta}:$, and therefore $\phi_>^{\rm op}(x) = -\frac{2M^2}{\pi}\,:\partial\theta\partial\tilde{\theta}:$.

Proceeding in the same way for the other observables for the two boundary conditions, we find the following scaling fields:

$$\phi_1^{\rm op} = \left(\frac{6}{\pi} - \frac{160}{3\pi^2} + \frac{1024}{9\pi^3}\right):\partial\theta\partial\tilde{\theta}:, \qquad \phi_>^{\rm op} = -\frac{2M^2}{\pi}\,:\partial\theta\partial\tilde{\theta}:, \tag{25}$$

$$\phi_1^{\rm cl} = -\frac{8}{\pi}\left(\frac{3}{4}-\frac{2}{\pi}\right)\left[:\partial\theta\partial\tilde{\theta}: + \frac{1}{16}M^2\,:\theta\tilde{\theta}:\right], \qquad \phi_>^{\rm cl} = \frac{M^2}{2\pi}\,:\theta\tilde{\theta}:\,. \quad (26)$$

These field identifications have been checked to be consistent with many multisite probabilities: two-site and three-site boundary/boundary probabilities as well as two-site and three-site mixed boundary/bulk probabilities.

The massless limit is simply given by the limit $t \to 0$ in the MASM and $M \to 0$ in the field theory. In this limit, the fields $\phi_>^{\rm op}$ and $\phi_>^{\rm cl}$ are obviously null and the unit height fields for the two boundaries are identical up to a numerical factor. One may note that the latter are proportional to the holomorphic stress–energy tensor, and being descendants of the identity, they belong to a chiral representation $\mathcal{V}_0$ [13]. This is consistent with the fact that the only fields living on an open boundary are fields of $\mathcal{V}_0$, and that those living on a closed boundary belong to an $\mathcal{R}_0$ representation, which contains $\mathcal{V}_0$ as subrepresentation [16, 17].

4. Spanning tree representation of recurrent configurations

For the other height variables, the situation is not as easy. Although having a height 1 or a height 2 at a given site does not seem to make much difference, the counting of the corresponding recurrent configurations is technically much more complicated for a height 2 (or 3 or 4) than for a height 1. The defect matrix method no longer works[2], and the only practical alternative seems to be the use of spanning trees. One then clearly sees the difference: in terms of spanning trees, a height 1 is characterized by a local property of the tree around the reference site, while the other heights are characterized by non-local properties of trees [4].

As mentioned earlier, the rooted spanning tree is defined on $\mathcal{L}^\star$, the lattice $\mathcal{L}$ augmented by the sink site, at which the tree is rooted. All sites i of $\mathcal{L}$ are connected by Δ_{ii} bonds to other sites: $-\Delta_{ij}$ bond(s) connecting i to j and $\sum_{j\in\mathcal{L}}\Delta_{ij}$ bond(s) connecting i to the root. With these definitions, the Kirchhoff theorem asserts that the number of rooted spanning trees on the graph $\mathcal{L}^\star$ defined by the matrix Δ is equal to $\mathcal{N} = \det\Delta$, precisely the number of recurrent configurations.

As a rooted spanning tree is a connected graph containing no loop, every site i is connected to the root by a unique path. A site j is said to be a predecessor of the site i if the path from j to the root passes through i, or equivalently, if j lies on a branch growing from i. A site i which has no predecessor is called a leaf (the end of a branch).

Priezzhev first and then Ivashkevich used the correspondence between recurrent configurations and spanning trees to compute respectively the one-site probabilities in the plane, and the one- and two-site probabilities on the boundary, open or closed, of the upper half-plane. For the one-site probabilities at i_0, they decomposed the set of recurrent configurations into subsets S_a, where S_a contains the recurrent configurations which remain allowed for any height $h_{i_0} \geqslant a$ and which are forbidden otherwise. These subsets S_a can be characterized in terms of rooted spanning trees and their cardinal can be computed using classical results in graph theory. As we will see, they decomposed local tree diagrams as sums of non-local diagrams. This system is invertible without further input for i_0 on a boundary, but is not for i_0 in the bulk. So the calculation of probabilities for sites in the bulk is more complicated.

For the two-site probabilities, Ivashkevich used a similar decomposition of the recurrent configurations into subsets S_{ab}. This decomposition however raises certain questions, and will not be used here. Instead we set up a particular one-to-one map between recurrent configurations and the rooted spanning trees, based on the burning algorithm. In the case of

[2] Except a height 4 on an open boundary, which can be handled like a supercritical height.

single site probabilities, the mapping yields the same characterization in terms of trees as the S_a decomposition but is much more transparent in the case of multisite probabilities.

The burning algorithm, as we described in section 2 complemented with an ordering prescription, establishes a one-to-one mapping but with no clear correspondence between the height values at the reference sites and the bond arrangements of the trees around those sites (except for supercritical heights which are directly connected to the root of the tree). For example, depending on the recurrent configuration, a site with a height 4 can be a leaf on the tree or can support 1, 2 or 3 branches. To avoid this problem, we proceed in two steps as follows, assuming that none of the reference sites is supercritical.

First, we run the burning algorithm and let the fire propagate through the lattice until no more site is burnable but *preventing the reference sites from burning*. When this is done, one is left with a sublattice $\mathcal{L}_\mathrm{b}$ of burnt sites and a complementary sublattice $\mathcal{L}_\mathrm{u}$ of unburnt sites. The algorithm, using for example the ordering prescription of [9], yields at this stage the part of the spanning tree on $\mathcal{L}_\mathrm{b}$. The other part $\mathcal{L}_\mathrm{u}$ is eventually burnable too and is actually burnt in the second step. By definition, none of the reference sites is burnt yet, and a certain number of them, at least one, is burnable. Those which are burnable are burnt simultaneously, and trigger the fire propagation through $\mathcal{L}_\mathrm{u}$, thereby completing the spanning tree to the whole lattice. So the complete tree is made of two pieces, a subtree $\mathcal{T}_\mathrm{b}$ on $\mathcal{L}_\mathrm{b}$, and another $\mathcal{T}_\mathrm{u}$ on $\mathcal{L}_\mathrm{u}$. The subtree $\mathcal{T}_\mathrm{u}$ itself may have several roots which are among the reference sites those which were burnable and which set fire to the whole of $\mathcal{L}_\mathrm{u}$. It is at those sites that $\mathcal{T}_\mathrm{u}$ is grafted to $\mathcal{T}_\mathrm{b}$ to make the full tree $\mathcal{T}$. As we will see, only the shape of the unburnt sublattice $\mathcal{L}_\mathrm{u}$ is used to characterize the height of the reference sites.

This slightly modified burning algorithm establishes a well-defined correspondence between spanning trees and heights of the reference sites in the critical as well as in the massive Abelian sandpile. Let us see how this works for the single-site probabilities, and how it allows us to compute the two-site height correlations where one of the two heights is equal to 1 or is supercritical. At this stage we will be able to identify the boundary fields corresponding to all heights. In the following section, we will compute other two-site and three-site correlations to confirm these identifications.

Let us consider a configuration of the MASM on a square lattice $\mathcal{L}$, and let us focus on a fixed site i_0, the reference site. We will take $\mathcal{L}$ to be the upper half-plane, but what follows applies to any sort of portion of $\mathbb{Z}^2$, bounded or unbounded.

- If the height at i_0 is supercritical, then i_0 is set afire by the root (is burnt at time 1). Thus all trees corresponding to those configurations have a bond connecting the root and i_0. The probability that i_0 is supercritical is thus

$$P[i_0 \text{ is supercritical}] = \frac{\mathcal{N}_{\star,i_0}}{\mathcal{N}}, \tag{27}$$

  where $\mathcal{N} = \det \Delta$ and $\mathcal{N}_{\star,i_0}$ is the number of different spanning trees which 'use' one of the t bonds between the root and i_0. One way to compute $\mathcal{N}_{\star,i_0}$ is to modify the toppling matrix by removing the connections between i_0 and its nearest neighbours on $\mathcal{L}$ so that i_0 has connections only to the root. Then $\mathcal{N}_{\star,i_0} = \det \Delta'$ with $\Delta' = \Delta + S^{(i_0)}$ and the finite-dimensional defect matrix given by $S^{(i_0)}_{i_0 i_0} = t - \Delta_{i_0 i_0}$, $S^{(i_0)}_{i_0 i_\ell} = S^{(i_0)}_{i_\ell i_0} = 1$ for i_ℓ the nearest neighbours of i_0, and zero elsewhere. A simpler way is however to compute $\mathcal{N} - \mathcal{N}_{\star,i_0}$, the number of trees which do not use the bonds between i_0 and the root. This can be done by removing precisely these bonds and leads to the one-dimensional defect matrix $\bar{S}^{(i_0)}$ of the previous section, with the result given in (14).

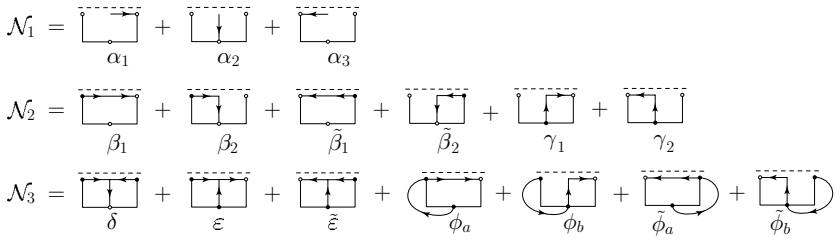

Figure 1. Non-local diagrams contributing to the one-site probabilities.

The same arguments apply to a height 4 at an open boundary site. The only difference is that such sites have $t + 1$ connections to the root, so that

$$P_4 = \frac{1}{t}\frac{\mathcal{N}_{\star,i_0}}{\mathcal{N}} = \Delta^{-1}_{i_0 i_0}, \qquad \text{for} \quad i_0 \text{ on open boundary.} \tag{28}$$

- If the height at i_0 is less than or equal to the number of nearest neighbours on $\mathcal{L}$, we use the burning algorithm to define a partition $\mathcal{L} = \mathcal{L}_{\mathrm{b}} \cup \mathcal{L}_{\mathrm{u}}$ as explained above. As one looks here at one-site probabilities, there is only one reference site, so that in the sublattice $\mathcal{L}_{\mathrm{u}} = \mathcal{L}_{i_0}$, i_0 is the only burnable site after all sites of $\mathcal{L}_{\mathrm{b}}$ have been burnt. It is therefore the root of the subtree $\mathcal{T}_{\mathrm{u}} = \mathcal{T}_{i_0}$. The height at i_0 can now be related to the properties of the subtree $\mathcal{T}_{i_0}$.
  If $\mathcal{L}_{i_0}$ contains only the site i_0, then h_{i_0} can take any of the values $1, 2, \ldots, n_{i_0}$, where $n_{i_0} = 3$ or 4 is the number of nearest neighbours of i_0. The full tree $\mathcal{T}$ is simply obtained by connecting i_0 to $\mathcal{T}_{\mathrm{b}}$ through one of the n_{i_0} bonds connecting i_0 to its nearest neighbours, so that i_0 is a leaf on $\mathcal{T}$ (i_0 must be connected to a nearest neighbour in $\mathcal{L}$ and not to the root, since it catches fire from one of them). If one denotes by $\mathcal{N}_1$ the number of spanning trees on $\mathcal{L}$ where i_0 is a leaf grown on one its neighbours, then

$$P_1 = \frac{\mathcal{N}_1}{n_{i_0}\mathcal{N}}. \tag{29}$$

  If $\mathcal{L}_{i_0}$ contains one nearest neighbour of the site i_0, the value of the height at i_0 must be in the set $\{2, \ldots, n_{i_0}\}$ (it cannot be 1 since otherwise i_0 would not be burnable and could not set $\mathcal{L}_{i_0}$ afire). There are now $n_{i_0} - 1$ possibilities of connecting $\mathcal{T}_{i_0}$ to $\mathcal{T}_{\mathrm{b}}$, one for each nearest neighbour of i_0 in $\mathcal{L}_{\mathrm{b}}$. They correspond to the height values compatible with the burning algorithm and thus the height 2 probability reads

$$P_2 = \frac{\mathcal{N}_1}{n_{i_0}\mathcal{N}} + \frac{\mathcal{N}_2}{(n_{i_0} - 1)\mathcal{N}}, \tag{30}$$

  where $\mathcal{N}_2$ is the number of spanning trees where i_0 has exactly one predecessor among its nearest neighbours.
  The higher height probabilities can be determined by the same arguments,

$$P_k = P_{k-1} + \frac{\mathcal{N}_k}{(n_{i_0} - k + 1)\mathcal{N}}, \qquad P_0 = 0, \qquad k = 1, \ldots, n_{i_0}, \tag{31}$$

  where $\mathcal{N}_k$ is the number of spanning trees $\mathcal{T}$ on $\mathcal{L}$ in which i_0 has exactly $k-1$ predecessors among his neighbours.

One sees that the computation of the various one-site probabilities requires the calculation of the numbers $\mathcal{N}_k$. If the lattice $\mathcal{L}$ is the discrete upper half-plane, and for i_0 a site on the boundary, figure 1 describes the types of trees which contribute to the different $\mathcal{N}_k$.

These diagrams represent the restriction of trees to four sites, namely the reference site i_0 and its three neighbours (the dashed line represents the border of $\mathcal{L}$, pictured as the lower half-plane!). The arrows indicate the direction of the path towards the root (opposite to the fire propagation line). The black dots are the nearest neighbours which are predecessors of i_0, the white dots are those which are not. Those diagrams labelled by identical greek letters contribute the same amount to the corresponding $\mathcal{N}_k$. The tilded letters refer to diagrams which are the mirror images of the diagrams with untilded letters.

The diagrams in figure 1 represent non-local constraints on the compatible trees. The presence of an arrow between i_0 and one or more neighbours is a local constraint, because it only means that the tree has to use specific bonds. But for a neighbour to be a predecessor or not is a non-local property, and enumerating the relevant trees is trickier. For the trees contributing to $\mathcal{N}_3$ for instance, one sees that a nearest neighbour, call it i_1, of i_0 can be a predecessor of i_0 because i_1 is connected to i_0 through the nearest neighbour bond (i_1 catches fire directly from i_0, like in δ, ε and $\tilde{\varepsilon}$), or through a long path around the lattice (i_1 catches fire after a long sequence of burnings, long after i_0 got burnt, like in ϕ and $\tilde{\phi}$).

Various classes of non-local diagrams in figure 1, with their constraints on predecessorships, sum up to local diagrams, where these constraints are relaxed and only local arrow configurations are imposed. As the local diagrams are easily calculable by toppling matrix adjustments, this yields linear relations among the non-local contributions. For a generic position of the reference site i_0, the linear system is not invertible and is not sufficient to compute the non-local contributions. The crucial observation made by Ivashkevich in [5] was to note that it actually becomes invertible if i_0 is on a boundary, which allows us to reduce the non-local contributions to local calculations (this statement will have to be qualified in the case of two-site insertions). Indeed the relations read explicitly [5] (as we consider the heights 1, 2 and 3 only, we do not need to distinguish the diagrams for closed and open boundaries, which only make a difference through the proper toppling matrix to be used in the explicit local computations; at the same time, that also makes the number of equations smaller)

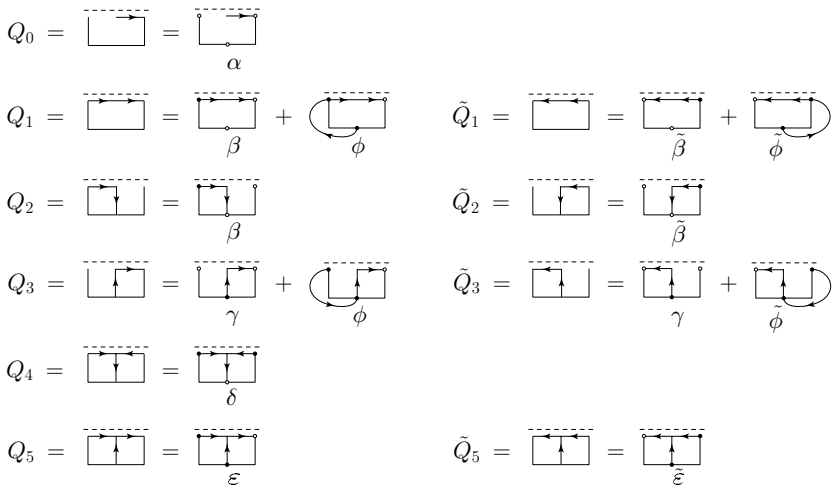

(32)

The four equations on the right are clearly obtained from the corresponding four on the left by a mirror symmetry about the reference site i_0. As the toppling matrix is invariant under that symmetry, the three tilded diagrams contribute the same amount as the untilded ones, $\tilde{\beta} = \beta, \tilde{\varepsilon} = \varepsilon, \tilde{\phi} = \phi$, as do the tilded and the untilded local diagrams. Thus the four

equations on the right are redundant, and one is left with the linear system on the left. This system is manifestly invertible for the six non-local contributions, denoted α, β, γ, δ, ε and ϕ.

Let us note that the non-local diagrams α, β, δ and ε turn out to be entirely local, because the arrow configurations make the predecessorship properties redundant. As the height 1 probability P_1 is given solely in terms of α, its computation is purely local. This remains true for any multisite height 1 probabilities and for arbitrary positions, in the bulk or on boundaries.

The Kirchoff theorem allows the local diagrams to be computed by the defect matrix method. The presence, resp. the absence, of an arrow from i to j means that one counts all trees which contain, resp. do not contain, that oriented bond. One defines a new toppling matrix Δ' by setting to $-\epsilon$ the i, j entry if the $i \to j$ bond is to be used in the tree, and to 0 if that bond is not to be used; moreover the diagonal entries of Δ'_{ii} should remain equal to the number of bonds going out from i. Then if n bonds are to be used, the determinant of Δ' will contain a highest degree term ϵ^n whose coefficient is the number of trees which precisely use the given n bonds in the prescribed direction (see for instance [4]).

Writing as before $\Delta' = \Delta + B$, one finds for Q_4 in the closed case

$$B = \begin{pmatrix} -3-t+\epsilon & 1 & 1-\epsilon & 1 \\ 1-\epsilon & -1+\epsilon & 0 & 0 \\ 1 & 0 & -1 & 0 \\ 1-\epsilon & 0 & 0 & -1+\epsilon \end{pmatrix}, \tag{33}$$

($-4-t+\epsilon$ as first entry in the open case), and, in the critical limit,

$$\frac{Q_4}{\mathcal{N}} = \frac{\delta}{\mathcal{N}} = \lim_{\epsilon\to\infty} \frac{1}{\epsilon^3} \det[\mathbb{I} + \Delta^{-1}B] = \begin{cases} \frac{1}{\pi} - \frac{1}{4} & \text{on closed boundary,} \\ \frac{(3\pi-8)^3}{9\pi^3} & \text{on open boundary.} \end{cases} \tag{34}$$

The calculation of the other five local diagrams and then the inversion of the linear system yields the values of $\mathcal{N}_1, \mathcal{N}_2$ and $\mathcal{N}_3$, and in turn of P_1, P_2 and P_3. In the critical limit, one recovers the numbers given in [5].

In order to identify the height boundary fields, we need two-site correlations involving the boundary heights 2 and 3. Again the simplest is to look at the correlations of a boundary height 2 or 3 with a known boundary variable, namely a height 1 or a supercritical height value. The advantage is that the latter are already known from the previous section, but more importantly, they correspond to local defect matrix insertions. This makes the above formalism, useful to compute one-site probabilities, essentially valid.

Because one can force a site i_0 to have height 1 or to be supercritical by modifying the toppling matrix by $\Delta \longrightarrow \Delta(i_0) = \Delta + B^{(i_0)}$ or $\Delta + S^{(i_0)}$ (or better $\Delta + \bar{S}^{(i_0)}$), the two-site probabilities $P[h_{i_0} = 1 \text{ or supercr.}, h_{j_0} = 2 \text{ or } 3]$ can be viewed as one-site probabilities for the height at j_0 but with the toppling matrix $\Delta(i_0)$ to account for the constraint at i_0. Then the above method remains completely valid provided we replace Δ by the appropriate $\Delta(i_0)$, itself to be modified by matrices like in (33) in order to compute local diagrams[3]. If one does that and uses $\Delta(i_0)$ as the normalizing toppling matrix, one is actually computing the conditional probability for having a 2 or a 3 at j_0 conditioned on having a height 1 or a supercritical height at i_0. To get the joint probabilities, one simply multiplies the final answers by $P\big[h_{i_0} = 1\big]$ or $P[h_{i_0} = \text{supercr.}]$.

The non-local diagrams contributing to the numbers $\mathcal{N}_k$ remain as in figure 1. However the tilded and the untilded diagrams no longer contribute equally because the mirror image about j_0 spoils the constraint at i_0, and does not leave the toppling matrix $\Delta(i_0)$ invariant.

[3] To keep the decompositions of the $\mathcal{N}_k$ in terms of the non-local diagrams as in figure 1, the site i_0 should not be too close to j_0.

Therefore it is the full system (32) that needs be solved. It is overdetermined as it involves ten equations for only nine unknowns, but the number of equations is reduced by one due to the following identity

$$\tilde{Q}_1 + Q_2 + Q_3 = Q_1 + \tilde{Q}_2 + \tilde{Q}_3, \tag{35}$$

satisfied for all values of t as a simple consequence of the fact that the inverse of $\Delta(i_0)$ satisfies a discrete Poisson equation. The procedure is otherwise identical to that for the one-site probabilities.

For the open boundary, the boundary joint probabilities of a site with height 2, 3 or 4 and a site with height 1 or with a supercritical height all have the same form as two unit heights on the boundary. It means the same field identification up to a numerical factor:

$$\phi_2^{\mathrm{op}} = \left(-\frac{18}{\pi} + \frac{400}{3\pi^2} - \frac{2048}{9\pi^3}\right) :\partial\theta\partial\tilde{\theta}:, \tag{36}$$

$$\phi_3^{\mathrm{op}} = \left(\frac{14}{\pi} - \frac{80}{\pi^2} + \frac{1024}{9\pi^3}\right) :\partial\theta\partial\tilde{\theta}:, \tag{37}$$

$$\phi_4^{\mathrm{op}} = -\frac{2}{\pi} :\partial\theta\partial\tilde{\theta}:. \tag{38}$$

The last line is easily obtained from (28), which implies $\phi_4^{\mathrm{op}} = \frac{1}{M^2}\phi_>^{\mathrm{op}}$.

For the closed boundary, the correlations involving a height 2 or 3 have a more complicated structure. For example, one finds (with $m = |i_0 - j_0|$)

$$P\big[h_{i_0} > 3, h_{j_0} = 2\big] = \frac{t^2}{\pi^2}\left[\frac{2}{\pi}K_0^2(m\sqrt{t}) - \left(3 - \frac{12}{\pi}\right)K_0'^2(m\sqrt{t}) - \frac{1}{2}K_0(m\sqrt{t})K_0''(m\sqrt{t})\right] + \cdots \tag{39}$$

$$P\big[h_{i_0} > 3, h_{j_0} = 3\big] = \frac{t^2}{\pi^2}\left[\frac{1}{4}K_0^2(m\sqrt{t}) - \frac{4}{\pi}K_0'^2(m\sqrt{t}) + \frac{1}{2}K_0(m\sqrt{t})K_0''(m\sqrt{t})\right] + \cdots \tag{40}$$

where the dots stand for order t^3 terms. These results and the corresponding ones for $h_{i_0} = 1$ are compatible with the following field assignments for the heights 2 and 3:

$$\phi_2^{\mathrm{cl}} = \left(\frac{6}{\pi} - \frac{24}{\pi^2}\right) :\partial\theta\partial\tilde{\theta}: + \frac{1}{2\pi} :\theta\partial\partial\tilde{\theta}: + \left(\frac{1}{8\pi} - \frac{1}{\pi^2}\right) M^2 :\theta\tilde{\theta}:, \tag{41}$$

$$\phi_3^{\mathrm{cl}} = \frac{8}{\pi^2} :\partial\theta\partial\tilde{\theta}: - \frac{1}{2\pi} :\theta\partial\partial\tilde{\theta}: - \frac{1}{4\pi}M^2 :\theta\tilde{\theta}:. \tag{42}$$

This identification is in this case not unique, since the field theory is invariant under $\theta \to \tilde{\theta}$ and $\tilde{\theta} \to -\theta$. One could in particular change $:\theta(\partial\partial\tilde{\theta}):$ for $:(\partial\partial\theta)\tilde{\theta}:$, which are different fields since their correlation contains a logarithm while their self-correlations do not. If one requires that the sum $\phi_1^{\mathrm{cl}} + \phi_2^{\mathrm{cl}} + \phi_3^{\mathrm{cl}}$ be zero in the massless limit, then the same choice for one of the two fields must be made for both ϕ_2^{cl} and ϕ_3^{cl}. The correlations computed in the next section confirm this. Note that the sum of fields $\phi_1^{\mathrm{cl}} + \phi_2^{\mathrm{cl}} + \phi_3^{\mathrm{cl}} + \phi_>^{\mathrm{cl}}$ vanishes identically. The similar sum in the open case, $\phi_1^{\mathrm{op}} + \phi_2^{\mathrm{op}} + \phi_3^{\mathrm{op}} + \phi_4^{\mathrm{op}} + \phi_>^{\mathrm{op}}$, vanishes at the critical point only, because the dimension of $\phi_>^{\mathrm{op}}$ does not match the dimension of the universal terms of the other fields.

At this stage, all boundary height fields for the massive Abelian sandpile model have been determined. To have more checks on the field identifications, we compute in the following section, all two-site and some three-site height correlations.

5. Higher boundary correlations

In the previous section we have seen that the multisite probabilities where only one reference site i_0 has a height value in $\{2, 3\}$ can be computed from the diagrams listed in figure 1 by using a toppling matrix properly decorated by defect matrices to account for height constraints (height 1 or supercritical) at the other sites. The calculation of multisite probabilities where two reference sites i_0 and j_0 have a height value in $\{2, 3\}$ leads naturally to pairs of such diagrams, one at i_0, the other at j_0. However the situation becomes technically more complex because sites in the diagram at i_0 can be predecessors of j_0 and/or the other way round. So the topology of the spanning trees can be more complicated and their counting more difficult.

Let us first consider the two-site probabilities $P_{ab} = P\big[h_{i_0} = a, h_{j_0} = b\big]$ for a, b in $\{2, 3\}$ and where i_0 and j_0 are on the boundary of the upper half-plane. We start the burning algorithm as explained in section 4 without ever burning the sites i_0 and j_0, and until no other sites than those two are burnable. This yields a sublattice $\mathcal{L}_{\mathrm{u}} = \mathcal{L}_{i_0 j_0}$ of unburnt sites, which subsequently catches fire either from i_0 or from j_0, or from both if they are both burnable. In turn the fire propagation on $\mathcal{L}_{i_0 j_0}$ defines a subtree $\mathcal{T}_{\mathrm{u}} = \mathcal{T}_{i_0 j_0}$, rooted at i_0, or at j_0, or at both sites. The full tree $\mathcal{T}$ is made up of the subtree $\mathcal{T}_{\mathrm{b}}$ living on the sublattice of burnt sites, to which $\mathcal{T}_{i_0 j_0}$ is grafted at i_0 and/or j_0.

The restriction of any tree to the neighbourhood of a reference site looks like one of the non-local diagrams shown in figure 1. So one can visualize the restriction to the two neighbourhoods by a pair of such diagrams. Using the same labelling as in figure 1, we will denote the pairs of diagrams by pairs of Greek letters (with indices), the first one for the diagram around i_0, the other for the diagram at j_0. In obvious notation, a pair of Greek letters belong to a certain set $\mathcal{N}_k \times \mathcal{N}_l$. As we did in section 4 for the one-site probabilities, we have to compute which probabilities P_{ab} a pair of diagrams contributes to.

For one-site probabilities, we know from section 4 that the diagrams in $\mathcal{N}_k$ contribute equally to the probabilities P_a for $k \leqslant a \leqslant 3$. Indeed the three diagrams $\alpha_1, \alpha_2, \alpha_3$ of $\mathcal{N}_1$ are obtained from each other by changing the arrow around the reference site. The change converts a tree which is compatible with a diagram α_i into a tree which is compatible with another diagram α_j, and this fact shows that the number of trees compatible with a diagram α_i does not depend on i, namely $\alpha_1 = \alpha_2 = \alpha_3$ or $\mathcal{N}_1 = 3\alpha$. As the position of the arrow determines univocally the height value, the three probabilities P_1, P_2, P_3 get an equal contribution $\mathcal{N}_1/3\mathcal{N}$ from the diagrams in $\mathcal{N}_1$. The same is true of the six diagrams in $\mathcal{N}_2$. They come in pairs (β_1, β_2), $(\tilde{\beta}_1, \tilde{\beta}_2)$, (γ_1, γ_2), where the diagrams within a pair are related by changing the direction of the arrow coming out from the reference site. The same arguments as above show that $\beta_1 = \beta_2$, $\tilde{\beta}_1 = \tilde{\beta}_2$, $\gamma_1 = \gamma_2$, and that P_2, P_3 receive an identical contribution $\beta + \tilde{\beta} + \gamma = \mathcal{N}_2/2\mathcal{N}$ from the diagrams in $\mathcal{N}_2$. For $\mathcal{N}_3$, each diagram is on its own and contributes to P_3.

In the case of two-site probabilities, the same arguments would show that the diagrams in $\mathcal{N}_k \times \mathcal{N}_l$ contribute equally to the probabilities P_{ab} for $k \leqslant a \leqslant 3, l \leqslant b \leqslant 3$, provided one can prove that changing the direction of an arrow in the way recalled above in either diagram, or in both diagrams, turns a compatible tree into a compatible tree of the same class. Because the two diagrams can now be linked by fire paths, this is no longer guaranteed, and actually fails in a few cases, pictured in figure 2.

On the first line of figure 2, one sees for instance that the diagram denoted by A_3 is a pair $\gamma_2\beta_1$. It is linked in such a way that when one changes the arrow in β_1, one obtains a well-defined tree (noted A_2) compatible with a pair $\tilde{\phi}_b\beta_2$. If one changes in A_3 the arrow of γ_2, one obtains the diagram A_1, of the type $\gamma_1\phi_a$. Changing the arrow of γ_2 and of β_1 introduces a loop, and so cannot contribute to a two-site probability. The trees compatible

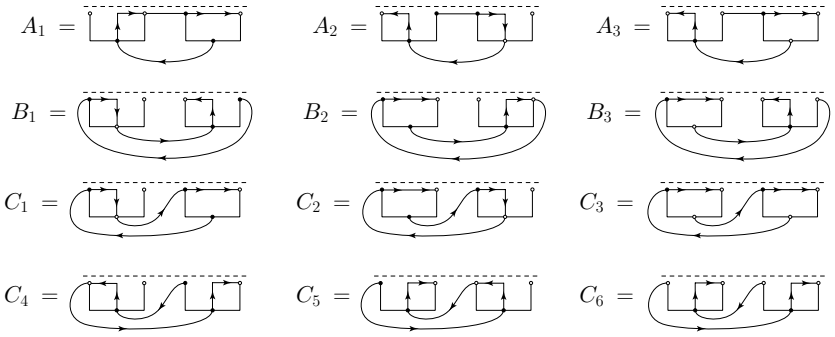

Figure 2. Non-local diagrams representing spanning trees which have anomalous behaviour under a local change of arrow around i_0 and/or j_0. The mirror diagrams must be added to have the complete list of such diagrams.

with the diagrams A_1, A_2 and A_3 are related by local changes of arrow, but belong to different classes, namely $\mathcal{N}_2 \times \mathcal{N}_3$, $\mathcal{N}_3 \times \mathcal{N}_2$ and $\mathcal{N}_2 \times \mathcal{N}_2$. There should normally be a fourth diagram, in $\mathcal{N}_3 \times \mathcal{N}_3$, but which does not exist as a tree.

It is not difficult to see that the misbehaviour with respect to arrow changes can only be of the type shown by the triplet (A_1, A_2, A_3). When the two diagrams are tied in a special way by the fire paths, one change of arrow in a diagram in $\mathcal{N}_2 \times \mathcal{N}_2$ sends it to a diagram in $\mathcal{N}_2 \times \mathcal{N}_3$ or $\mathcal{N}_3 \times \mathcal{N}_2$, and two arrow changes introduce a loop.

Figure 2 shows four triplets of diagrams where this peculiar behaviour occurs. Diagrams labelled by the same capital letter are in equal number, since the numbers of compatible trees are equal. The 12 diagrams shown in figure 2 and the mirror diagrams (not shown in figure 2), obtained by exchanging the diagram at i_0 with the reflected one at j_0 and vice versa, make the complete list of misbehaved diagrams. We will denote the mirror diagrams with tildes.

The two-step burning algorithm allows us to determine which probability each diagram contributes to. In the diagram A_1 for instance, the subtree $\mathcal{T}_{i_0 j_0}$ catches fire from the eastern neighbour of j_0. It is thus burnable at a time where only one of its neighbours is burnt, and so must have a height 3. The other reference site i_0 is not burnable at the time $\mathcal{T}_{i_0 j_0}$ catches fire despite the fact that its western neighbour was burnt, which implies that its height is at most 2. When i_0 is burnable, it has two burnt neighbours and one southern unburnt neighbour, meaning that its height must be 2. Thus A_1 contributes to P_{23}. One finds similarly that the first column in figure 2 contributes to P_{23}, the second column to P_{32}, and the last column to P_{33}.

We define $[\mathcal{N}_k \times \mathcal{N}_l]$ to be the set of trees in $\mathcal{N}_k \times \mathcal{N}_l$ which do not have this sort of misbehaviour under a local change of arrow. The set $\mathcal{N}_k \times \mathcal{N}_l$ is equal to $[\mathcal{N}_k \times \mathcal{N}_l]$ except in the following three cases:

$$\mathcal{N}_2 \times \mathcal{N}_2 = [\mathcal{N}_2 \times \mathcal{N}_2] + A_3 + B_3 + C_3 + C_6 + \tilde{A}_3 + \tilde{B}_3 + \tilde{C}_3 + \tilde{C}_6, \tag{43}$$

$$\mathcal{N}_2 \times \mathcal{N}_3 = [\mathcal{N}_2 \times \mathcal{N}_3] + A_1 + B_1 + C_1 + C_4 + \tilde{A}_2 + \tilde{B}_2 + \tilde{C}_2 + \tilde{C}_5, \tag{44}$$

$$\mathcal{N}_3 \times \mathcal{N}_2 = [\mathcal{N}_3 \times \mathcal{N}_2] + A_2 + B_2 + C_2 + C_5 + \tilde{A}_1 + \tilde{B}_1 + \tilde{C}_1 + \tilde{C}_4. \tag{45}$$

The trees in $[\mathcal{N}_k \times \mathcal{N}_l]$ contribute equally to the probabilities $P_{ab}, k \leqslant a \leqslant 3$ and $l \leqslant b \leqslant 3$, while those compatible with the diagrams of figure 2 must be handled separately. One obtains

$$P_{22} = P_{12} + P_{21} - P_{11} + \frac{[\mathcal{N}_2 \times \mathcal{N}_2]}{4\mathcal{N}}, \tag{46}$$

$$P_{23} = P_{13} + P_{22} - P_{12} + \frac{[\mathcal{N}_2 \times \mathcal{N}_3]}{2\mathcal{N}} + \frac{1}{\mathcal{N}}[A_1 + B_1 + C_1 + C_4 + \tilde{A}_2 + \tilde{B}_2 + \tilde{C}_2 + \tilde{C}_5], \tag{47}$$

$$P_{32} = P_{22} + P_{31} - P_{21} + \frac{[\mathcal{N}_3 \times \mathcal{N}_2]}{2\mathcal{N}} + \frac{1}{\mathcal{N}}[A_2 + B_2 + C_2 + C_5 + \tilde{A}_1 + \tilde{B}_1 + \tilde{C}_1 + \tilde{C}_4], \tag{48}$$

$$\begin{aligned} P_{33} = {} & P_{23} + P_{32} - P_{22} + \frac{\mathcal{N}_3 \times \mathcal{N}_3}{\mathcal{N}} + \frac{1}{\mathcal{N}}[A_3 + B_3 + C_3 + C_6 + \tilde{A}_3 + \tilde{B}_3 + \tilde{C}_3 + \tilde{C}_6] \\ & - \frac{1}{\mathcal{N}}[A_1 + A_2 + B_1 + B_2 + C_1 + C_2 + C_4 + C_5 + \text{mirrors}]. \end{aligned} \tag{49}$$

The subtracted term in P_{33} is due to the fact that the parts of P_{23}, P_{32} related to the misbehaved diagrams in figure 2 (first and second columns) do not contribute to P_{33}.

The sets $[\mathcal{N}_k \times \mathcal{N}_l]$ will be further partitioned in classes labelled by a pair of diagrams, *f.i.* $[\mathcal{N}_2 \times \mathcal{N}_2] = [\beta_1\beta_1] + [\beta_1\beta_2] + \cdots$. One will recall that the cardinal of a class does not depend on the *numerical* indices attached to diagrams, so that $|[\beta_1\beta_1]| = |[\beta_1\beta_2]| = |[\beta_2\beta_1]| = |[\beta_2\beta_2]|$, and so on. Replacing however ϕ_a by ϕ_b in a class does not necessarily conserve the cardinal of that class, *f.i.* $|[\beta\phi_a]| \neq |[\beta\phi_b]|$. The two-site probabilities can be computed if the numbers of trees in these subclasses and of those compatible with the non-local diagrams of figure 2 can be calculated.

As for the one-site probabilities, we can decompose each pair of local diagrams as a sum of non-local ones. We have for example,

$Q_{1,1} =$ 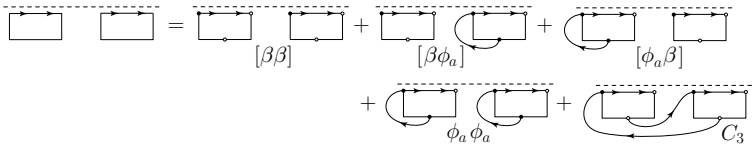

(50)

$Q_{2,3} =$ 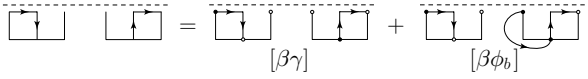

(51)

As such, the linear system one obtains in this way is underdetermined. Let us proceed to the counting in the general case, that is, when heights equal to 1 or supercritical heights are inserted at other places than i_0 and j_0. In this situation, the full system must include all pairs of local diagrams (for example, one would have the equation $Q_{1,1}$ and its mirror image $\tilde{Q}_{1,1}$).

There are 81 equations like (50) and (51), since every such equation is a pair of local diagrams, chosen from the nine diagrams appearing on the last five lines of equation (32). There are 9 independent variables for the classes of $[\mathcal{N}_2 \times \mathcal{N}_2]$ (pairs of elements in $\{\beta, \tilde{\beta}, \gamma\}$ since the indices are irrelevant), 21 variables for the classes of $[\mathcal{N}_2 \times \mathcal{N}_3]$ and $[\mathcal{N}_3 \times \mathcal{N}_2]$, and 49 variables for $\mathcal{N}_3 \times \mathcal{N}_3$. To these one must add the four variables A, B, C and $\tilde{C}$, for the diagrams of figure 2 (one can show that $A = \tilde{A}$ and $B = \tilde{B}$).

In total, one has a linear system of 81 equations for 104 variables. It is actually worse because the equations are not all independent, due to some non-trivial identities among local diagrams (as in (35)). It is however possible to compute the probabilities in terms of a reduced number of variables.

In the calculation of the one-site probabilities, the non-local diagrams ϕ_a and ϕ_b each brought an equal contribution, because for any tree compatible with ϕ_a, there is a tree compatible with ϕ_b and vice versa. Thus a single variable ϕ was used for the two diagrams.

The substitution of ϕ_a by ϕ_b in a pair of diagrams does not always conserve the number of trees, so that the number of independent variables for pairs of diagrams involving a ϕ cannot

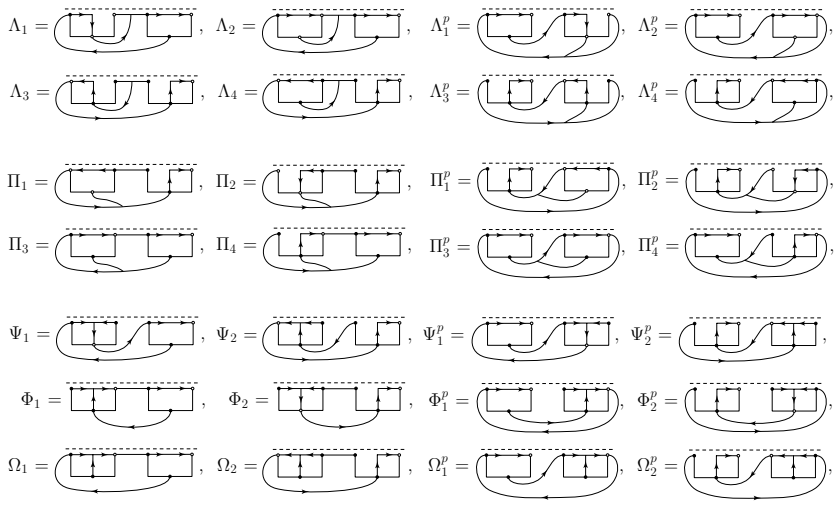

Figure 3. Non-local diagrams representing spanning trees which have anomalous behaviour under the substitution of ϕ_a by ϕ_b, or of ϕ_b by ϕ_a. The superscript p indicates that the two diagrams at the reference sites have been permuted. All mirror diagrams must be added.

be reduced by a factor 2. However, one may separate in $[\mathcal{N}_2 \times \mathcal{N}_3]$, $[\mathcal{N}_3 \times \mathcal{N}_2]$ and $\mathcal{N}_3 \times \mathcal{N}_3$ the trees for which the substitution is allowed from the others, as we did above regarding the change of arrows.

It turns out that this is useful because only a reduced number of pairs of diagrams misbehave under the change $\phi_a \leftrightarrow \phi_b$. Up to mirror symmetry, they are all given in figure 3.

For instance, the two diagrams Λ_1 and Λ_2 are pairs $[\beta_2\phi_a]$ and $[\beta_1\phi_a]$, contained in the set $[\mathcal{N}_2 \times \mathcal{N}_3]$. The change $\phi_a \to \phi_b$ in Λ_1 requires a change of direction in the path going from the southern neighbour of j_0 through i_0 and back to j_0, which is not possible. The pair Π_1 and Π_2 corresponds to the diagrams $[\tilde{\beta}_1\phi_b]$ and $[\tilde{\beta}_2\phi_b]$, also in $[\mathcal{N}_2 \times \mathcal{N}_3]$. Their permuted versions belong to $[\mathcal{N}_3 \times \mathcal{N}_2]$, while all the other diagrams in figure 3 are in $\mathcal{N}_3 \times \mathcal{N}_3$. The diagrams whose labels differ only by the numerical subscript contribute equally, so $\Lambda_1 = \Lambda_2$ but $\Lambda_1 \neq \tilde{\Lambda}_1$.

If one denotes by curly brackets the sets of trees which are closed under the change $\phi_a \leftrightarrow \phi_b$, one can write

$$[\mathcal{N}_2 \times \mathcal{N}_3] = \{[\mathcal{N}_2 \times \mathcal{N}_3]\} + \Lambda_1 + \Lambda_2 + \Pi_1 + \Pi_2 + \tilde{\Lambda}_1^p + \tilde{\Lambda}_2^p + \tilde{\Pi}_1^p + \tilde{\Pi}_2^p, \tag{52}$$

$$[\mathcal{N}_3 \times \mathcal{N}_2] = \{[\mathcal{N}_3 \times \mathcal{N}_2]\} + \Lambda_1^p + \Lambda_2^p + \Pi_1^p + \Pi_2^p + \tilde{\Lambda}_1 + \tilde{\Lambda}_2 + \tilde{\Pi}_1 + \tilde{\Pi}_2, \tag{53}$$

$$\mathcal{N}_3 \times \mathcal{N}_3 = \{\mathcal{N}_3 \times \mathcal{N}_3\} + \Lambda_3 + \Lambda_4 + \Pi_3 + \Pi_4 + \Phi_1 + \Phi_2 + \Psi_1 + \Psi_2 + \Omega_1 + \Omega_2 + \text{mirrors and permuted.} \tag{54}$$

The diagrams $\Lambda_1 + \Lambda_2$, $\Pi_1 + \Pi_2$ and the permuted tilded versions contribute equally to P_{23} and P_{33}, since they are in $[\mathcal{N}_2 \times \mathcal{N}_3]$. The diagrams $\Lambda_1^p + \Lambda_2^p$, $\Pi_1^p + \Pi_2^p$ (and the permuted tilded versions) contribute equally to P_{32} and P_{33}, whereas all the others contribute to P_{33} only. Thus the expressions for the two-site probabilities become

$$P_{22} = P_{12} + P_{21} - P_{11} + \frac{[\mathcal{N}_2 \times \mathcal{N}_2]}{4\mathcal{N}}, \tag{55}$$

$$P_{23} = P_{13} + P_{22} - P_{12} + \frac{\{[\mathcal{N}_2 \times \mathcal{N}_3]\}}{2\mathcal{N}} + \frac{1}{2\mathcal{N}}\big[2A_1 + 2B_1 + 2C_1 + 2C_4 + 2\tilde{A}_2 + 2\tilde{B}_2 + 2\tilde{C}_2 + 2\tilde{C}_5 + \Lambda_1 + \Lambda_2 + \Pi_1 + \Pi_2 + \tilde{\Lambda}_1^p + \tilde{\Lambda}_2^p + \tilde{\Pi}_1^p + \tilde{\Pi}_2^p\big], \tag{56}$$

$$P_{33} = P_{23} + P_{32} - P_{22} + \frac{\{\mathcal{N}_3 \times \mathcal{N}_3\}}{\mathcal{N}} + \frac{1}{\mathcal{N}}[A_3 + B_3 + C_3 + C_6 - A_1 - A_2 - B_1 - B_2 - C_1 - C_2 - C_4 - C_5 + \text{mirrors}] + \frac{1}{\mathcal{N}}[\Lambda_3 + \Lambda_4 + \Pi_3 + \Pi_4 + \Psi_1 + \Psi_2 + \Phi_1 + \Phi_2 + \Omega_1 + \Omega_2 + \text{mirrors and permuted}]. \tag{57}$$

The variables entering these expressions can be determined from the same linear system as above, expressed in terms of the new variables. For instance, the first equation becomes

$Q_{1,1} =$ 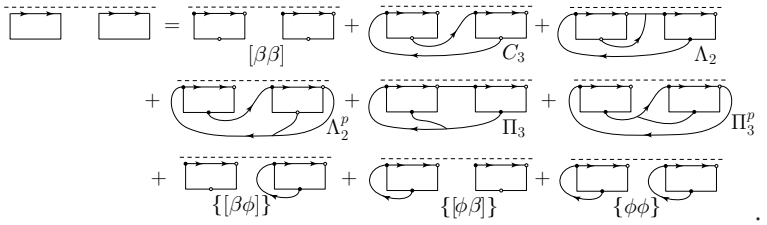 (58)

The number of equations is the same, but we have fewer variables. The new sets $\{[\mathcal{N}_2 \times \mathcal{N}_3]\}$, $\{[\mathcal{N}_3 \times \mathcal{N}_2]\}$ and $\{\mathcal{N}_3 \times \mathcal{N}_3\}$ have respectively 15, 15 and 25 variables, to which 20 extra variables are added for the diagrams in figure 3 and their mirror images. So there are 88 variables, constrained by 81 linear equations, of which 73 only are linearly independent. The system is still underdetermined but unexpectedly allows us to determine enough variables to compute the probabilities without further work.

First one can show, by suitably combining the independent equations, that $[A + B + C + \tilde{C}]/\mathcal{N}$ is equal to a combination of local diagrams which turns out to be subdominant, of order t^3 for both an open or a closed boundary (order m^{-6} at the critical point, where m is the distance between i_0 and j_0). As the four quantities are positive by construction, it means that each of them is at least of order t^3, and can be neglected. Thus one relation determines four variables. Once these four variables are eliminated, one is left with a system of 72 independent equations for 84 variables.

Being independent, the 72 equations allow us to determine 72 combinations of variables. The point is that one can choose these 72 combinations in such a way that the probabilities can be fully expressed in terms of them only, thereby making knowledge of the other 12 combinations useless. Alternatively, one may choose to solve the linear system for 72 variables, which then become functions of the remaining 12. When inserted in the probabilities, all dependences in the 12 unknowns drop out completely. The set of the 12 variables that the system cannot determine is not unique, but a possible choice is $\{\Psi, \Psi^p, \Lambda^p, \Pi^p, \Phi^p, \Omega^p + \text{mirrors}\}$.

The counting of variables and equations is different when there are no insertions at other places than i_0 and j_0 since the mirrored equations are redundant. One finds that the linear system is again not invertible, but is nonetheless sufficient to compute all two-site boundary probabilities. They have been computed in the massive model to the dominant order t^2, which yields the universal terms.

For an open boundary, we found that none of the diagrams in figure 3 contributes to the dominant order, being at least of order t^3. The probabilities P_{22}, P_{23} and P_{33} have the same

form $t^2[K_0''(m\sqrt{t}) - K_0(m\sqrt{t})]^2$ at dominant order, and only differ by their normalizations. These have been checked to be in agreement with the identifications obtained in section 4.

The case of a closed boundary is a bit more complicated. In this case the diagrams of figure 3 contribute to order t^2 (as we have seen above, none of the diagrams of figure 2 contribute, irrespective of the boundary condition), and the connected probabilities read

$$P_{22} = t^2 \left(-\frac{4}{\pi^4} K_0(m\sqrt{t})^2 - \left(\frac{48}{\pi^4} - \frac{12}{\pi^3} \right) K_0'(m\sqrt{t})^2 + \frac{2}{\pi^3} K_0(m\sqrt{t}) K_0''(m\sqrt{t}) \right.$$
$$\left. - \left(\frac{144}{\pi^4} - \frac{72}{\pi^3} + \frac{37}{4\pi^2} \right) K_0''(m\sqrt{t})^2 + \left(\frac{12}{\pi^3} - \frac{3}{\pi^2} \right) K_0'(m\sqrt{t}) K_0'''(m\sqrt{t}) \right) + \cdots \tag{59}$$

$$P_{23} = t^2 \left(-\frac{1}{2\pi^3} K_0(m\sqrt{t})^2 + \left(\frac{8}{\pi^4} - \frac{3}{\pi^3} + \frac{3}{4\pi^2} \right) K_0'(m\sqrt{t})^2 \right.$$
$$- \left(\frac{1}{\pi^3} - \frac{1}{8\pi^2} \right) K_0(m\sqrt{t}) K_0''(m\sqrt{t}) + \left(\frac{48}{\pi^4} - \frac{12}{\pi^3} + \frac{1}{4\pi^2} \right) K_0''(m\sqrt{t})^2$$
$$\left. - \left(\frac{8}{\pi^3} - \frac{3}{2\pi^2} \right) K_0'(m\sqrt{t}) K_0'''(m\sqrt{t}) \right) + \cdots \tag{60}$$

$$P_{33} = t^2 \left(-\frac{1}{16\pi^2} K_0(m\sqrt{t})^2 + \frac{2}{\pi^3} K_0'(m\sqrt{t})^2 - \frac{1}{4\pi^2} K_0(m\sqrt{t}) K_0''(m\sqrt{t}) \right.$$
$$\left. - \left(\frac{16}{\pi^4} + \frac{1}{4\pi^2} \right) K_0''(m\sqrt{t})^2 + \frac{4}{\pi^3} K_0'(m\sqrt{t}) K_0'''(m\sqrt{t}) \right) + \cdots . \tag{61}$$

Again they are in full agreement with the fields found in section 4.

We have also computed a few three-site probabilities, when one of the insertions is a height 1 or a supercritical height. Then the same system as above can be used, the only difference is that the Laplacian has to be decorated by a local defect matrix, and only affects the calculation of the local diagrams. We have found for instance the connected probability P_{212} to have a height 1 and two heights 2 on a closed boundary, all separated by large distances, at the critical point (the expressions for off-critical three-site probabilities are too long),

$$P_{212,\mathrm{conn}} = \frac{2}{\pi^3} \left(\frac{3}{4} - \frac{2}{\pi} \right) \left\{ \frac{1}{m_{12} m_{13}^2 m_{23}^3} + \frac{1}{m_{12}^3 m_{13}^2 m_{23}} + \frac{1}{\pi^2} \frac{(6\pi - 24)^2}{m_{12}^2 m_{13}^2 m_{23}^2} + \frac{6\pi - 24}{\pi} \right.$$
$$\left. \times \left[\frac{1}{m_{12} m_{13}^3 m_{23}^2} + \frac{1}{m_{12}^2 m_{13}^3 m_{23}} + \frac{1}{m_{12}^3 m_{13} m_{23}^2} + \frac{1}{m_{12}^2 m_{13} m_{23}^3} \right] \right\} + \mathcal{O}\left(m_{ij}^{-8} \right) \tag{62}$$

where m_{ij} is the distance between the ith and jth site. The connected probability is equal to $P_{212,\mathrm{conn}} = P_{212} - P_2 P_{12} - P_{22} P_1 - P_{21} P_2 + 2P_2^2 P_1$. The previous formula for P_{212} is equivalent to that found by Jeng [7], but allows for a more direct comparison with the field theoretic result, as the various terms correspond to specific Wick contractions.

6. Conclusion

We have addressed the question of the field identification of the boundary height variables in the two-dimensional dissipative Abelian sandpile model, for the two boundary conditions open and closed. The height variables can take four or five different values depending on the type of boundary they lie on. On an open boundary, a height may be equal to 1, 2, 3, 4, or

be supercritical (larger than 4), while on a closed boundary, the allowed values are 1, 2, 3 and supercritical (larger than 3). In the scaling limit, each of these nine values is described by a specific field ϕ_i, which is a local combination of two massive free Grassmannian scalars θ and $\tilde{\theta}$, themselves belonging to the massive perturbation of a conformal field theory with central charge $c = -2$.

On an open boundary, the fields ϕ_i only differ by their normalization and read explicitly

$$\phi_1 = \left(\frac{6}{\pi} - \frac{160}{3\pi^2} + \frac{1024}{9\pi^3}\right) :\partial\theta\partial\tilde{\theta}:, \qquad \phi_2 = \left(-\frac{18}{\pi} + \frac{400}{3\pi^2} - \frac{2048}{9\pi^3}\right) :\partial\theta\partial\tilde{\theta}:, \tag{63}$$

$$\phi_3 = \left(\frac{14}{\pi} - \frac{80}{\pi^2} + \frac{1024}{9\pi^3}\right) :\partial\theta\partial\tilde{\theta}:, \qquad \phi_4 = -\frac{2}{\pi} :\partial\theta\partial\tilde{\theta}:, \tag{64}$$

$$\phi_> = -\frac{2M^2}{\pi} :\partial\theta\partial\tilde{\theta}:. \tag{65}$$

where the fundamental fields θ and $\tilde{\theta}$ are subject to the Dirichlet boundary condition $\theta = \tilde{\theta} = 0$.

On a closed boundary, the fields θ and $\tilde{\theta}$ satisfy the Neumann boundary condition $(\partial - \bar{\partial})\theta = (\partial - \bar{\partial})\tilde{\theta} = 0$, and the four scaling fields are different

$$\phi_1 = -\frac{8}{\pi}\left(\frac{3}{4} - \frac{2}{\pi}\right)\left[:\partial\theta\partial\tilde{\theta}: + \frac{1}{16}M^2 :\theta\tilde{\theta}:\right], \tag{66}$$

$$\phi_2 = \left(\frac{6}{\pi} - \frac{24}{\pi^2}\right) :\partial\theta\partial\tilde{\theta}: + \frac{1}{2\pi} :\theta\partial\partial\tilde{\theta}: + \left(\frac{1}{8\pi} - \frac{1}{\pi^2}\right) M^2 :\theta\tilde{\theta}:, \tag{67}$$

$$\phi_3 = \frac{8}{\pi^2} :\partial\theta\partial\tilde{\theta}: - \frac{1}{2\pi} :\theta\partial\partial\tilde{\theta}: - \frac{1}{4\pi}M^2 :\theta\tilde{\theta}:, \qquad \phi_> = \frac{M^2}{2\pi} :\theta\tilde{\theta}:. \tag{68}$$

In the massless limit $M \to 0$, the non-dissipative sandpile model is recovered, and the supercritical variables $\phi_>$ disappear. The remaining three or four height variables have two-point correlations which all decay like r^{-4}.

Acknowledgments

We would like to thank Monwhea Jeng for instructive discussions and comparisons of our respective methods. They led us to realize that our early calculations had overlooked some diagrams, which however had no effect on the end results.

References

[1] Cardy J L 1987 Conformal invariance *Phase Transitions and Critical Phenomena* vol 11 ed C Domb and J L Lebowitz (New York: Academic)
[2] Bak P, Tang C and Wiesenfeld K 1987 *Phys. Rev. Lett.* **59** 381
[3] Majumdar S N and Dhar D 1991 *J. Phys. A: Math. Gen.* **24** L357
[4] Priezzhev V B 1994 *J. Stat. Phys.* **74** 955
[5] Ivashkevich E V 1994 *J. Phys. A: Math. Gen.* **27** 3643
[6] Mahieu S and Ruelle P 2001 *Phys. Rev.* E **64** 066130
[7] Jeng M 2003 The four height variables of the Abelian sandpile model *Preprint* cond-mat/0312656
Jeng M 2004 The four height variables, boundary correlations, and dissipative defects in the Abelian sandpile model *Preprint* cond-mat/0405594
[8] Dhar D 1990 *Phys. Rev. Lett.* **64** 1613
[9] Majumdar S N and Dhar D 1992 *Physica* A **185** 129

[10] Tsuchiya T and Katori M 2000 *Phys. Rev.* E **61** 1183
[11] Gurarie V 1993 *Nucl. Phys.* B **410** 535
[12] Kausch H 2000 *Nucl. Phys.* B **583** 513
[13] Gaberdiel M R and Kausch H 1999 *Nucl. Phys.* B **538** 631
[14] Brankov J G, Ivashkevich E V and Priezzhev V B 1993 *J. Phys. I France* **3** 1729
[15] Jeng M 2004 Conformal field theory correlations in the Abelian sandpile model *Preprint* cond-mat/0407115
[16] Ruelle P 2002 *Phys. Lett.* B **539** 172
[17] Piroux G and Ruelle P 2004 JSTAT P10005